



Modeling of localized neutral particle sources in 3D edge plasmas

M.V. Umansky ^{a,*}, T.D. Rognlien ^a, M.E. Fenstermacher ^a, M. Borchardt ^b,
A. Mutzke ^b, J. Riemann ^b, R. Schneider ^b, L.W. Owen ^c

^a Lawrence Livermore National Laboratory, Livermore, CA 94550, USA

^b Max-Planck-Institut für Plasmaphysik, D-17491 Greifswald, Germany

^c Oak Ridge National Laboratory, Oak Ridge, TN 37830, USA

Received 27 May 2002; accepted 20 September 2002

Abstract

A 3D fluid neutral model is added to the 3D plasma transport code BoRiS. The neutral model includes equations for parallel momentum and collisional perpendicular diffusion. This makes BoRiS an integrated plasma-neutral model suitable for a variety of applications. Results are presented for the distribution of neutrals from a localized gas source in the National Compact Stellarator Experiment geometry.

© 2003 Elsevier Science B.V. All rights reserved.

PACS: 52.40.H; 52.65.H; 52.55.H

Keywords: 3D edge plasma; Neutral transport; Stellarator

1. Introduction

The 3D code BoRiS [1] is being developed as a comprehensive numerical tool for modeling of edge plasmas in 3D geometry, in particular for stellarators. BoRiS has a fully 3D fluid plasma model, and it is becoming capable of reproducing 1D and 2D plasma solutions [2] from the 2D edge codes such as B2 [3] and UEDGE [4]. However a plasma model alone is insufficient to address many problems in the edge plasma where the neutral particles strongly influence the plasma; thus a neutral model is needed to allow for self-consistent plasma-neutral calculations. Although the most accurate treatment of neutral transport is provided by the Monte Carlo methods, a fluid neutral model, such as the one implemented in UEDGE [5,6], usually makes a reasonably good approximation for the neutrals in the edge plasmas when the neutral mean free path, λ_N , is

small compared to the characteristic spatial scale length, L . The fluid neutrals model has certain advantages compared to Monte Carlo models from the numeric point of view: it has no statistical noise, it can be efficiently coupled with a plasma fluid model, and it is much faster; so the fluid neutrals model is the method of choice when λ_N is sufficiently small. A comparison of a fluid neutrals model that is built into the UEDGE code and a Monte Carlo model [7] demonstrated that general features of the results are quite similar for a certain range of plasma parameters and geometric configurations relevant to divertor plasmas. In the present paper we describe implementation of the fluid neutral model in BoRiS and its application to the National Compact Stellarator Experiment (NCSX) stellarator geometry.

2. Neutral transport model

2.1. Model description

In the presented model the neutral fluid consists of atoms with temperature equal to the ion temperature,

* Corresponding author. Tel.: +1-925 4226040/6041; fax: +1-925 4233484.

E-mail address: umansky@llnl.gov (M.V. Umansky).

which is determined from a summed ion-neutral thermal energy equation. We also solve the neutral density and the neutral momentum equations.

The neutral density equation is

$$\frac{\partial}{\partial t}(n_N) + \nabla \cdot (n_N \vec{V}_N) = -S_i + S_r, \quad (1)$$

where n_N is the neutral density, \vec{V}_N is the neutral flow velocity, and S_i , S_r stand for ionization and recombination sources, respectively.

For the neutral parallel momentum equation, we consider two options: the full Navier–Stokes equation and a reduced (diffusive) model.

The Navier–Stokes equation is

$$\begin{aligned} \frac{\partial}{\partial t}(mn_N V_{\parallel N}) + \nabla \cdot (mn_i \vec{V}_N V_{\parallel N} - \hat{\eta}_N \vec{\nabla} V_{\parallel N}) \\ = -\nabla_{\parallel} p_N + mn_i n_N K_{cx}(V_{\parallel i} - V_{\parallel N}) + mS_r V_{\parallel i} - mS_i V_{\parallel N}, \end{aligned} \quad (2)$$

where $V_{\parallel i}$ is the ion parallel flow velocity, $V_{\parallel N}$ is the neutral parallel flow velocity, m is the atom mass, n_i is the background plasma ion density, p_N is the neutral pressure, η_N is the neutral viscosity, and K_{cx} is the charge-exchange rate.

The diffusive approximation Eq. (3) corresponds to keeping only the pressure and charge-exchange terms in the Navier–Stokes equation

$$V_{\parallel N} = -D_N(\nabla_{\parallel} n_N/n_N + \nabla_{\parallel} T_i/T_i) + V_{\parallel i}, \quad (3)$$

where T_i is the ion-neutral temperature and D_N is the neutral diffusion coefficient, $D_N = T_i/(K_{cx} m n_i)$.

The perpendicular neutral velocity is always calculated in the diffusive approximation

$$V_{\perp N} = -D_N(\nabla_{\perp} n_N/n_N + \nabla_{\perp} T_i/T_i) + V_{\perp i}. \quad (4)$$

In the diffusive model, a flux limiting procedure is used for the particle flux, j_N

$$j_N \rightarrow j_N / \left[1 + \alpha \left(\frac{j_N}{n_N V_{T_i}/4} \right)^{\gamma} \right]^{1/\gamma}, \quad (5)$$

where typical parameter values used are $\alpha = 1$ and $\gamma = 2$. As flux limiting makes some correction for the kinetic effects, it generally improves the accuracy of the fluid model when the condition of small neutral mean free path, $\lambda_N \ll L$, is not very well satisfied.

2.2. Benchmark with UEDGE

To verify the performance of the fluid neutral model in BoRiS, we conduct a series of 1D and 2D benchmarks with the 2D edge code UEDGE. As the diffusive neutrals model in BoRiS is presently much more robust numerically than the Navier–Stokes model, in particular in complicated 2D and 3D geometry, we will present only the results from the diffusive model; a study of the Navier–Stokes model performance will be the subject of a future work. Fig. 1 shows the comparison of a calculation with BoRiS and UEDGE for neutral density distribution for a sample problem in a 2D box geometry. Neutral particles are assumed injected at a rate 1000 equivalent A/m through the inlet at the top boundary; at the remainder of the top boundary, the normal neutral flux is set zero, while on the other three sides of the box the neutral density is set at $1 \times 10^{14} \text{ m}^{-3}$. Plasma parameters are assumed constant with a temperature of 10 eV, density of $1 \times 10^{20} \text{ m}^{-3}$ and flow velocity of $V_{\parallel i} = 5 \times 10^4 \text{ m/s}$.

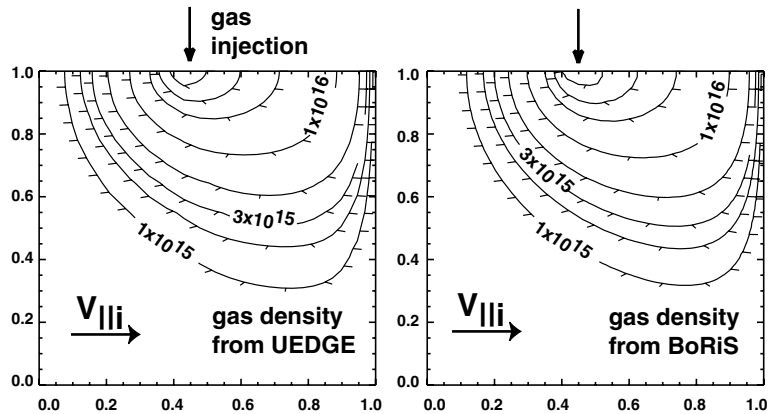


Fig. 1. Neutral density contours for the same test problem solved by UEDGE and BoRiS. The background plasma has density $1 \times 10^{20} \text{ m}^{-3}$, temperature 10 eV, and flow velocity $V_{\parallel i} = 5 \times 10^4 \text{ m/s}$. The box dimensions are $1 \times 1 \text{ m}$, and the neutrals are injected through the inlet at the top boundary at a rate of 1000 equivalent A/m. At the remainder of the top boundary the normal neutral flux is set zero, and on the other three sides of the box the neutral density is set at $1 \times 10^{14} \text{ m}^{-3}$.

Both BoRiS and UEDGE were used to solve this problem with the diffusive neutral model. Same models were used for the atomic physics rates: the charge-exchange cross-section was taken as constant, $\sigma_{\text{ex}} = 5 \times 10^{-19} \text{ m}^2$, recombination was set zero ($S_r = 0$), and for the ionization rate we used a simple analytic approximation which is reasonably accurate for the relevant range of temperature [3]

$$\frac{S_i}{n_e n_N} = 3 \times 10^{-14} \frac{(T_e/10)^2}{3 + (T_e/10)^2} \quad [\text{m}^3/\text{s}]. \quad (6)$$

In Eq. (6), T_e is the electron temperature in eV.

The resulting neutral density plumes shown in Fig. 1 are very similar, but not identical due to differences in the meshes and finite-differencing used.

3. Application to National Compact Stellarator Experiment geometry

3.1. Physical motivation

The NCSX [9] is being planned as a major new US fusion experiment. It is known that control of neutrals is essential for good plasma performance in stellarators [8]. The main sources of neutrals are plasma-facing components such as limiters and target plates. It is planned to install poloidal limiters on the inner side of the ‘bullet-like’ section [10], and the neutrals are assumed to originate at those locations. If poorly confined, the recycling neutrals can penetrate deep into the main plasma and cause large power loss by charge-exchange, radiation,

and convection. This is particularly an issue for NCSX where the core plasma width is rather small in the ‘banana-like’ toroidal sections. This motivates calculation of neutral penetration into the core plasma for NCSX geometry, assuming some model profiles of background plasma density and temperature.

3.2. Grid generation

As BoRiS uses magnetic coordinates [1], one needs first to calculate the magnetic coordinate representation for NCSX. A method for calculating the mapping between the real coordinates (R, Z, Φ_g) and the magnetic coordinates (s, θ, ϕ) from a given magnetic field using line tracing was developed by Boozer [11,12]. Here s , θ and ϕ correspond to the radial, poloidal-like and toroidal-like magnetic coordinates normalized to unity. We use actual magnetic field data [13] found for NCSX from magneto-hydrodynamic (MHD) free boundary calculations with numerical codes VMEC [14,15] and MFBE [16]. This magnetic field data correspond to the original design of NCSX with the average major radius $R_{\text{maj}} \approx 1.7 \text{ m}$. In Summer 2001, NCSX was redesigned and scaled down to $R_{\text{maj}} \approx 1.4 \text{ m}$ by applying a uniform scaling factor 0.82; we use this scaling factor for modeling of the NCSX reduced design configuration. We neglect the stochastic field regions found by line tracing outside of NCSX last closed magnetic surface (LCMS) [17] and consider only the inner part of NCSX flux tube where line tracing indicates existence of ‘good’ flux surfaces [17]. The metric data from the ‘good’ flux surfaces region are then extrapolated outside the LCMS to

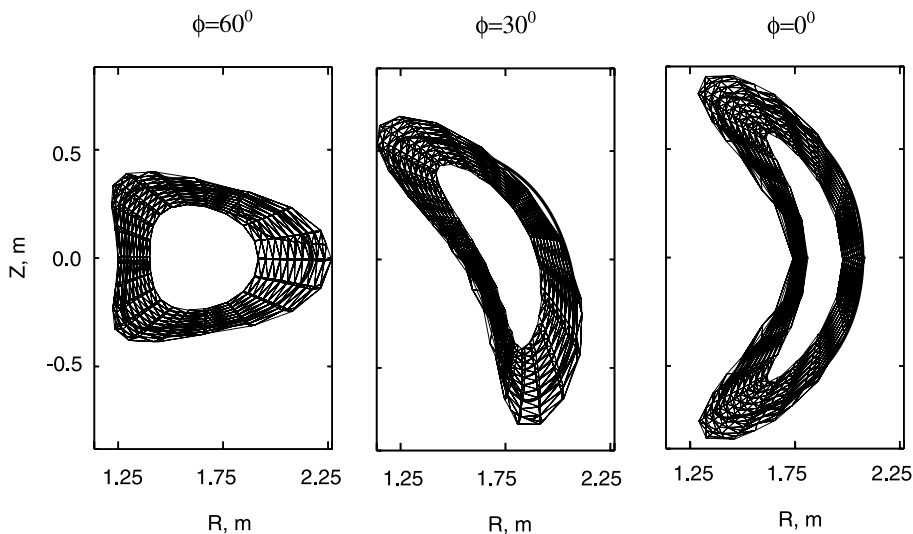


Fig. 2. Three toroidal cross-sections of the 3D grid used for NCSX calculations, corresponding to constant values of the geometric toroidal angle 60° , 30° , and 0° . For the reduced design of NCSX ($R_{\text{maj}} = 1.4 \text{ m}$) the grid is uniformly scaled down by a factor of 0.82. LCMS from MFBE calculations is shown by the thick line.

provide a model for NCSX geometry both inside and outside of LCMS. Using a line tracing method similar to [11,12], we calculate the magnetic coordinates for NCSX from the data. Then we use several leading Fourier amplitudes of this mapping to construct a simplified model of NCSX geometry which provides a good qualitative and quantitative match to the shape and dimensions of NCSX flux tubes, as shown in Fig. 2. This model of NCSX geometry is used in the calculations described below.

3.3. Code setup

The computational domain for these calculations represents one toroidal period of the NCSX flux tube region between two flux surfaces, where the outer surface represent the outer wall, and the inner surface is close enough to the magnetic axis to allow a simple boundary condition for the neutrals there. For the background plasma, we consider temperature and density profiles which depend only on the radial flux coordinate, s , with

$$\begin{aligned} T/T_0 = n/n_0 &= 2 - (3/2s)^2, & 0 \leq s \leq 2/3, \\ T/T_0 = n/n_0 &= e^{(2-3s)}, & 2/3 \leq s \leq 1, \end{aligned} \quad (7)$$

where the normalization parameters T_0 and n_0 are the LCMS values at $s = 2/3$ (see Fig. 3).

The boundary conditions for the neutrals are taken as follows: On the inner boundary of the domain ($s \approx 0$), a zero neutral flux condition is set since very few neutral particles typically penetrate that far into the plasma. The outer boundary ($s = 1$) also has a zero flux condition which represents a perfect wall, except for an area $0.4 \leq \theta$, $\phi \leq 0.6$ where a fixed neutral density $n_N =$

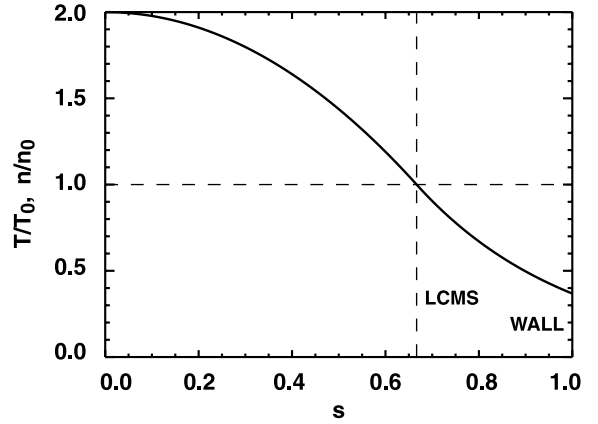


Fig. 3. Radial profiles of normalized density and temperature for the plasma used for the NCSX calculation.

$1 \times 10^{18} \text{ m}^{-3}$ is set. This region simulates a source of neutral gas localized at the inner mid-plane ($\theta = 0.5$) of the ‘bullet’ cross-section.

3.4. Calculation results

We calculate the 3D distribution of neutral density for two different plasma background temperature and density distributions: (a) $T_0 = 50 \text{ eV}$ and $n_0 = 1 \times 10^{19} \text{ m}^{-3}$, and (b) $T_0 = 50 \text{ eV}$ and $n_0 = 0.5 \times 10^{19} \text{ m}^{-3}$. The atomic physics rates are the same as in Section 2.2.

In Fig. 4 one can see contours of neutral density for three toroidal cross-sections for geometric toroidal angle values 60° , 30° and 0° . Note that neutral density is reduced by a factor on the order of ~ 1000 towards the ‘banana’ cross-section.

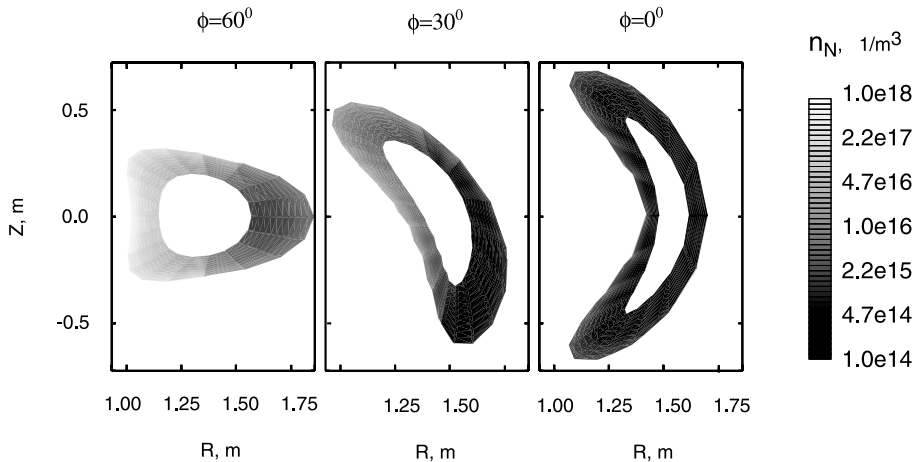


Fig. 4. Neutral density distribution for NCSX case (a) with plasma profiles using $T_0 = 50 \text{ eV}$ and $n_0 = 1 \times 10^{19} \text{ m}^{-3}$. Three toroidal cross-sections are shown corresponding to constant values of the geometric toroidal angle 60° , 30° , and 0° .

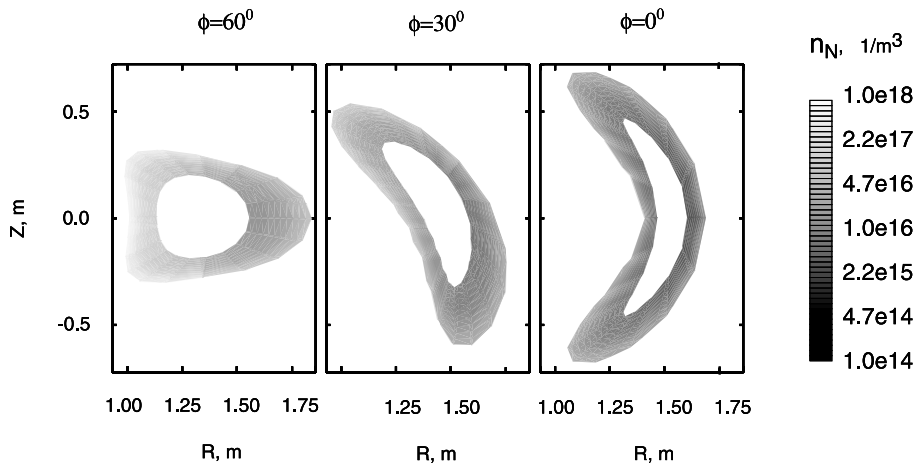


Fig. 5. Neutral density distribution for a plasma density 1/2 of that used for Fig. 4.

In Fig. 5, corresponding to case (b) with lower density of the background plasma, one can observe that the neutrals spread broader over the plasma, and the reduction towards the ‘banana’ cross-section is not as strong as in case (a), by a factor on the order of ~ 100 .

4. Conclusions

The BoRiS code has been supplemented with a fluid neutral model. This model has been tested against the UEDGE code in 1D and 2D setups. Applying BoRiS to neutral transport calculation in the NCSX stellarator geometry provides full 3D solutions which may have important consequences for NCSX design such as the possible need for baffles.

Acknowledgements

We would like to thank Dr A. Grossman (UCSD) for NCSX magnetic field data. This work is performed for USDOE by Univ. Calif. LLNL under contracts W-7405-ENG-48.

References

- [1] M. Borchardt et al., *J. Nucl. Mater.* 290–293 (2001) 546.
- [2] J. Riemann et al., Hierarchy tests of edge transport models (BoRiS, UEDGE), these Proceedings.
- [3] B.J. Braams, NET Report no. 68, 1987.
- [4] T.D. Rognlien et al., *J. Nucl. Mater.* 347–351 (1992) 196.
- [5] T.D. Rognlien et al., *Contrib. Plasm. Phys.* 34 (1994) 362.
- [6] F. Wising et al., *Contrib. Plasm. Phys.* 36 (1996) 136.
- [7] M.E. Rensink et al., *Contrib. Plasm. Phys.* 38 (1998) 325.
- [8] P. Grigull et al., EPS Conference, Madeira, Portugal, 18–22 June 2001.
- [9] G.H. Neilson et al., *Phys. Plasm.* 7 (2000) 1911.
- [10] P. Mioduszewski, NCSX Project Physics Meeting, 31 January 2002.
- [11] A.H. Boozer, *Phys. Fluids* 25 (1982) 520.
- [12] G. Kuo-Petravic et al., *J. Comput. Phys.* 51 (1983) 261.
- [13] A. Grossman, Private communication, 2001.
- [14] S.P. Hirshman et al., *Comput. Phys. Commun.* 43 (1986) 143.
- [15] S.P. Hirshman, D.K. Lee, *Comput. Phys. Commun.* 39 (1986) 161.
- [16] E. Strumberger, *Nucl. Fusion* 37 (1997) 19.
- [17] A. Koniges et al., Magnetic topology of a candidate NCSX plasma boundary configuration, *Nucl. Fusion*, submitted for publication.